

Enhancing Flood Impact Analysis through the Integration of Landsat and MODIS Imagery

Tran Vu Van Hoa¹, Nguyen Chi Thien¹, Truong Thanh Tung¹, Tuan Anh Nguyen^{*2}, Lam Bao Hoang³, Dang Thai Son³

²The SDCT Research Group, University of Transport Ho Chi Minh City, Vietnam

²University of Transport Ho Chi Minh City, Vietnam

³Ha Tinh Department of Construction, Ha Tinh Province, Vietnam

ARTICLE INFO

Article History:

Accepted: 15 April 2024

Published: 22 April 2024

Publication Issue :

Volume 11, Issue 2

March-April-2024

Page Number :

381-391

ABSTRACT

This article explores the efficacy of integrating Landsat and MODIS satellite imagery for comprehensive flood impact analysis. By employing advanced remote sensing technologies and sophisticated data processing techniques, this study offers a methodological framework that enhances the precision and depth of environmental analysis. The core methodology involves the systematic processing of satellite data, including radiometric and geometric corrections, combined with the use of analytical indices such as the Normalized Difference Water Index (NDWI) and the Enhanced Vegetation Index (EVI). These indices play a crucial role in accurately delineating water bodies and assessing the extent of flooding. The approach not only improves the reliability of flood mapping but also contributes to the broader understanding of environmental changes and aids in effective disaster management. Through this study, we demonstrate how strategic data integration can provide valuable insights for policymakers, enhancing responses to environmental crises.

Keywords: Remote Sensing, Flood Impact Analysis, Landsat and MODIS Integration, NDWI.

I. INTRODUCTION

This study employs cutting-edge satellite imagery from Landsat and MODIS to assess flood impacts, showcasing a sophisticated methodology centered around remote sensing technology [1, 2]. The distinct advantages of Landsat's high-resolution imagery combined with MODIS's ability to capture rapid temporal changes provide a robust framework for

detailed environmental analysis [3, 4]. Our research methodology is rigorously designed to utilize the strengths of each system to comprehensively monitor and analyze flood dynamics over large geographic areas.

Central to our approach is the advanced processing of Landsat and MODIS data, which involves several critical steps to ensure the highest data quality. For

Landsat, this includes the acquisition of spectral data, which is then subjected to radiometric and geometric corrections to adjust for any sensor and atmospheric anomalies, as well as satellite positioning errors. MODIS data, with its frequent revisits, complements this by providing timely updates on changing surface conditions, crucial during and after flood events.

Furthermore, our methodology employs sophisticated classification techniques to interpret the data accurately. This includes the use of the Normalized Difference Water Index (NDWI) to distinguish water from non-water features and the Enhanced Vegetation Index (EVI) to assess vegetation health, which is often impacted by flooding [5, 6]. These indices, alongside supervised classification methods using Maximum Likelihood algorithms, allow for detailed and accurate flood mapping and analysis [7, 8].

By integrating these approaches, our study not only enhances the understanding of flood mechanisms but also contributes to more effective flood management strategies [9, 10], aiding policymakers and local authorities in making informed decisions based on comprehensive environmental data.

II. MATERIAL AND METHOD

The research primarily makes use of satellite imagery from Landsat and MODIS, each offering unique advantages for environmental monitoring. Landsat images, renowned for their high-resolution capabilities, are instrumental in observing detailed surface characteristics and changes over time [4, 11]. This precision allows for an in-depth analysis of land use and environmental transformations, crucial for flood-related studies. On the other hand, MODIS images, with their higher temporal resolution but lower spatial accuracy compared to Landsat, are employed to capture frequent changes in surface conditions (Table I) [12, 13].

TABLE I

SPECTRAL CHANNELS OF MODIS IMAGES

Spectral channels	Wavelength (µm)	Spatial resolution
1	0.62 - 0.67	250
2	0.841 - 0.867	250
3	0.459 - 0.479	500
4	0.545 - 0.565	500
5	1.230 - 1.250	500
6	1.628 - 1.652	500
7	2.105 - 2.155	500

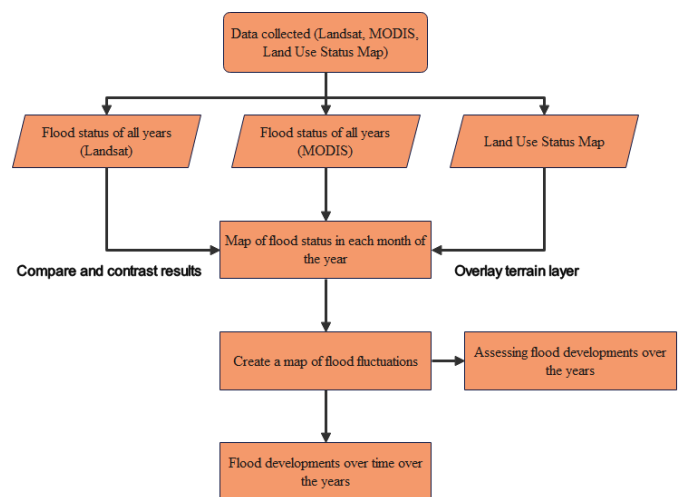


Figure 1: General diagram of research methodology

This is particularly useful for monitoring rapid variations in flood extents. The data set is further enriched with region-specific maps that delineate the current land use patterns in the Tu Giac Long Xuyen area. These maps are pivotal for correlating satellite observations with actual ground conditions, enhancing the accuracy of the flood analysis. Collectively, this integrated approach using varied data sources underpins the study's methodology, ensuring a comprehensive assessment of flood impacts and aiding in the development of effective flood management strategies (Figure 1).

Landsat image processing process

The processing of Landsat remote sensing images is a comprehensive procedure that begins with the acquisition of images across various spectral bands, captured and stored as digital numbers (DNs) by Landsat satellites. These images are subsequently made accessible through platforms such as the USGS Earth Explorer. Once acquired, the images undergo several critical preprocessing steps. Radiometric correction is applied to convert DN values into reflectance values, compensating for sensor-specific responses and atmospheric conditions to ensure the images accurately represent surface reflectance. Simultaneously, geometric correction aligns the image with geographic coordinates to rectify distortions caused by the satellite's positioning and the curvature of the Earth (Figure 2).

The method of mapping flood status is based on supervised classification

Sample regions of interest (ROI) with the following characteristics: Hydrosystems are light blue to dark blue, rivers are often linear, lakes and ponds are regional, Mixed types (not hydrosystems) have Regions This color includes vacant land, residential areas, roads, vegetation and industrial land [14, 15].

The section discusses the methodology for sampling Regions of Interest (ROI) and creating flood status maps using supervised classification techniques. This method leverages basic color combination principles of satellite imagery, utilizing primary color combinations including natural color, infrared, and pseudo color channels. Each combination serves a specific purpose: natural color (3-2-1) is used mainly for printing or as a background in database creation, providing a view akin to that from an airplane, which allows for the general identification of large-scale hydrological systems, roads, and urban areas. However, it may struggle with finer details such as small water bodies or minor roads [16]. The infrared combination (4-3-2) excels in interpreting surface features, traffic, and hydrology, allowing for clear differentiation between water bodies,

alluvial plains, and urban zones based on color distinctions. This method highlights vegetation in red due to strong reflection in the near-infrared channel, making it invaluable for ecological studies but potentially misleading in terms of natural color perception. The pseudo color combinations (5-4-3 or 7-4-2) enhance the visibility of hydrological and vegetative features by aligning color perception closer to human vision, making it easier to distinguish between different types of vegetation and land use [17, 18].

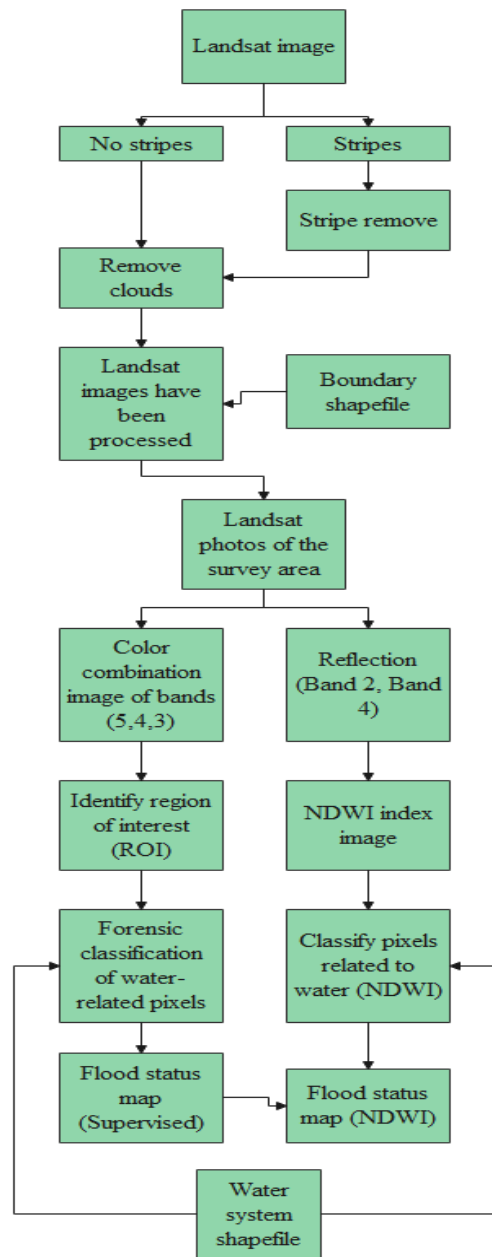


Figure 2: Landsat image processing process

In practice, the supervised classification (Maximum Likelihood) approach is employed to create detailed flood maps. This process involves identifying and classifying each pixel based on its spectral signature, which is compared against known categories in the ROI samples (Figure 3) [19]. These regions are preliminarily categorized based on their color attributes in imagery water bodies appear in shades of blue, while non-water mixed regions vary greatly in color, indicating features such as barren land, urban areas, or vegetation.

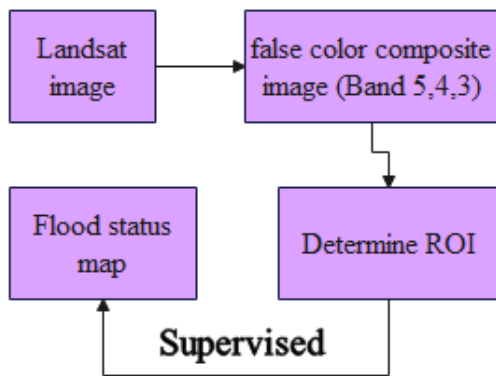


Figure 3: The process of mapping flood status by classification method (ROI)

Method of mapping flood status based on NDWI index

The Normalized Difference Water Index (NDWI) is a crucial tool in remote sensing for identifying water-related features in satellite imagery (Figure 4) [20, 21]. NDWI values range from -1 to +1, where pixels with values greater than 0 indicate the presence of water, effectively distinguishing flooded areas from non-flooded ones. Conversely, pixels with NDWI values less than 0 are indicative of non-water features, such as dry land or vegetated areas. This index is particularly useful in environmental studies for mapping and monitoring aquatic ecosystems, providing clear delineation between water bodies and other land cover types based on their spectral signatures [22].

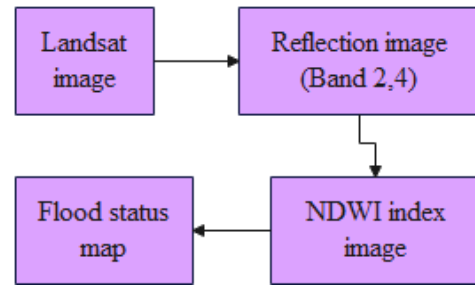


Figure 4: The process of mapping flood status by classification method (NDWI)

Modis image processing for flood mapping

The study utilizes the Enhanced Vegetation Index (EVI) as an alternative to the Normalized Difference Vegetation Index (NDVI) [23]. The EVI is calculated using the formula (1).

$$EVI = 2.5 * (NIR - RED) / [NIR + 6 * RED - 7.5 * BLUE + 1] \tag{1}$$

Where NIR represents near-infrared reflectance, RED is the reflectance in the red channel, and BLUE is the reflectance in the blue channel (Figure 5) [24-26].

Higher EVI values indicate denser vegetation cover, reflecting strong plant reflectivity, especially in bright color tones. Conversely, lower EVI values suggest sparse vegetation. EVI values may approach zero in areas with minimal or no vegetation and can even be negative in waterlogged regions.

The Land Surface Water Index (LSWI) [27, 28] indicates changes in surface water content and is derived from the formula (2).

$$LSWI = (NIR - SWIR) / (NIR + SWIR) \tag{2}$$

Where SWIR stands for short-wave infrared reflectance. An EVI value greater than 0.3 on MODIS images signifies pixels unrelated to water. Pixels with EVI values from 0.1 to 0.3 indicate mixed land areas (e.g., wetlands, water vegetation), and those ≤ 0.1 typically correspond to long-standing water bodies (e.g., rivers, lakes). The Differential Vegetation and Water Index (DVEL) is then constructed from EVI and

LSWI images, with DVEL values < 0.05 indicating water-related pixels [29, 30].

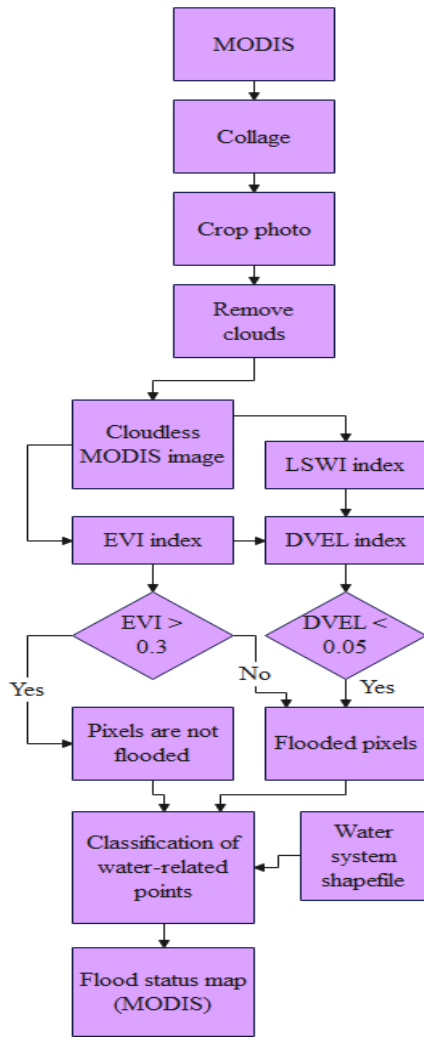


Figure 5: MODIS image processing to map flood status

Accuracy assessment methods

The assessment of classification accuracy using flood maps created from Landsat images (utilizing the NDWI index) is essential. These maps are compared with flood area data for the Tu Giac Long Xuyen based on water level measurements recorded at Chau Doc and Xuan To stations [31, 32]. Since Landsat images offer much higher spatial resolution than MODIS images, the flood maps derived from Landsat are more accurate than those created from MODIS images [8, 33]. Results analyzed from landsat images should be taken to evaluate the accuracy of results from MODIS image analysis.

III. RESULTS

Create flood status maps based on index images (ROI and NDWI) (Figure 6).

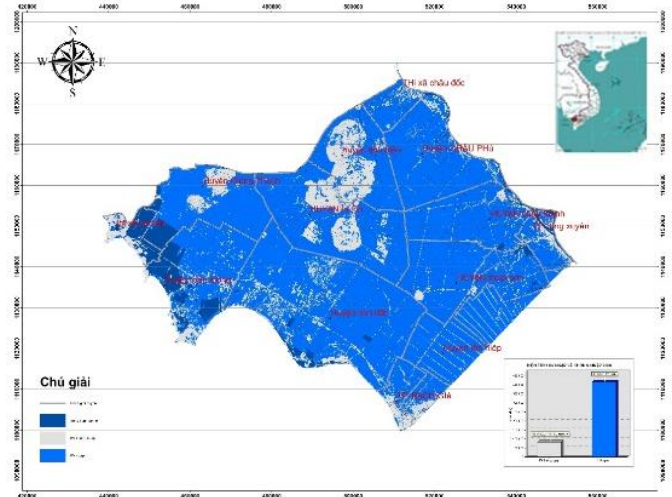


Figure 6: Map of flood status according to supervised classification method

Flood status map with post-classification accuracy (Kappa index and Overall Accuracy): Overall Accuracy = (1000/1092) = 91.5751%, Kappa Coefficient = 0.8282.

TABLE II
STATISTICS ON FLOOD AREA (SUPERVISED CLASSIFICATION)

FID	Class_Name	Area (ha)	%
0	Flooded areas	365304.8783	73.31813
1	Non-flooded areas	82715.29688	16.60129
2	Hydrosystem	50226.1217	10.08058
3	Total area	498246.2969	100

The flooded area is not too much, mostly the eastern areas of the Tu Giac Long Xuyen, except for Thoai Son Hau district, which does not appear to be flooded. The flooded area accounts for 38.96% of the entire area of the Tu Giac Long Xuyen region (Figure 7 and Figure 8).

NDWI index image (value from -1 to 1) for pixels with bright colors are pixels related to water. Through photos, the flooded area can be recognized as a whole.

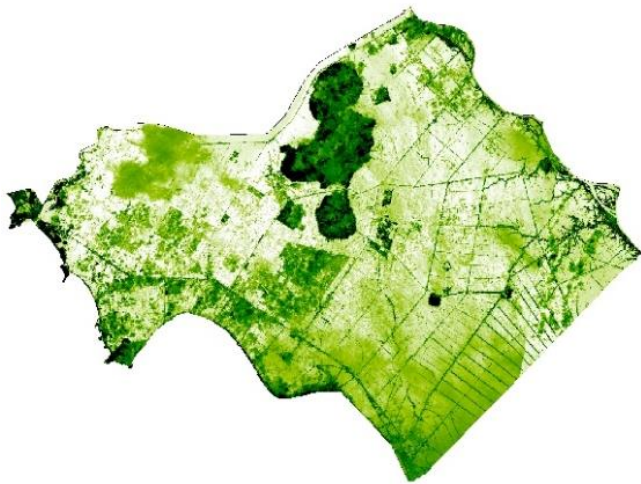


Figure 7: Photo of NDWI water difference index

Landsat image interpretation results (Table II and Table III).

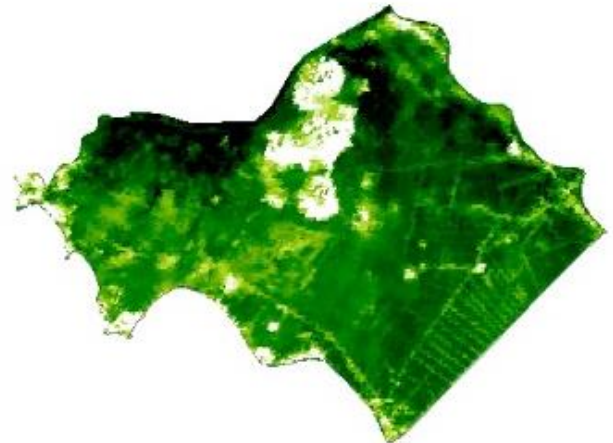


Figure 9: Cloudless EVI index image

EVI images reflect the state of vegetation at different times of the year, which is an important index in classification to assess the presence of vegetation and identify pixels related to water (Figure 9).

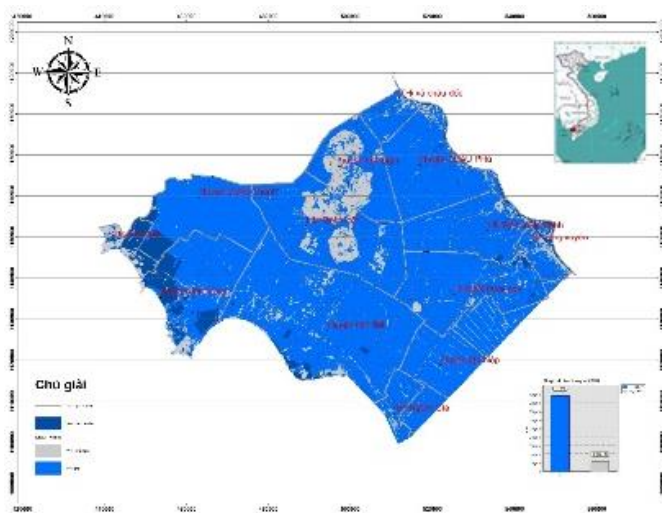


Figure 8: Map of flood status according to NDWI method

LSWI index images reflect the presence of water at different times of the year. The higher the LSWI value shows the stronger reflection of the water surface corresponding to the amount of water existing on the surface corresponding to the light tone, in contrast to places with little or no presence of water corresponding to the tone dark color (Figure 10).

TABLE III

STATISTICS ON FLOOD AREA (NDWI)

FID	Class_Name	Area (ha)	%
0	Flooded areas	390,144.88	78.303005
1	Non-flooded areas	57,879.20	11.616493
3	Hydrosystem	50226.1217	10.080502
4	Total area	498,250.20	100

In which the results of interpretation by supervised classification account for 73% of flooded areas and 16% of non-flooded areas. So there is a large correlation between the two methods, increasing the reliability of

LSWI images presented with dark tones represent high LSWI values corresponding to flooded areas, and with areas with little or no water presence corresponding to light-toned pixels. Through different levels of light and dark in the image, it is possible to see the change in water on the coating surface between the first months of the year compared to the last months of the year, creating a basis for classification (Figure 11).

Create flood status maps based on index images (EVI, DVEL and LSWI).

The main objects that need to be classified in the study are pixels related to water, so the two main objects that

need to be classified are flooded pixels (rivers, hydrological farming areas, rice fields, flowing water). flood overflow and flooded areas) and non-flooded pixels (forests, hills, bare land or vegetation cover.

Applying the method of creating flood status maps using EVI and DVEL index (Figure 12).

The flooded area and the area of rivers, canals, ponds and lakes almost completely occupy the Tgu Giac Long Xuyen region (accounting for nearly 96%). Areas that are not flooded are areas with high terrain (Table IV).

TABLE IV

FLOOD AREA STATISTICS IN FLOOD STATUS MAP CREATED FROM MODIS IMAGES

FID	Class_Name	Area (ha)	%
0	Mixture	6,225.27	1.244053
1	Non-flooded areas	16,851.40	3.367571
2	Flooded areas	427,276.88	85.38669
3	Hydrosystem	50226.12	10.03715
4	Total area	500,579.67	100



Figure 10: LSWI index image

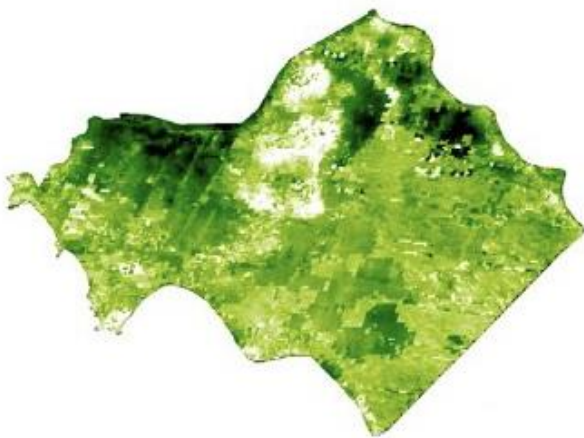


Figure 11: DVEL index image

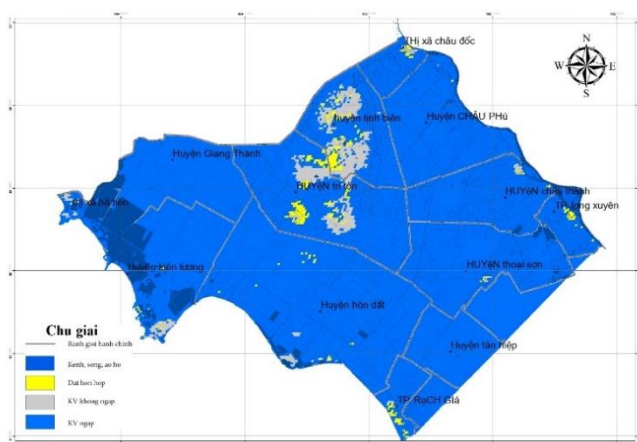


Figure 12: Flood status map created from MODIS images

Compare the interpretation results with monitoring data at Chau Doc measuring station.

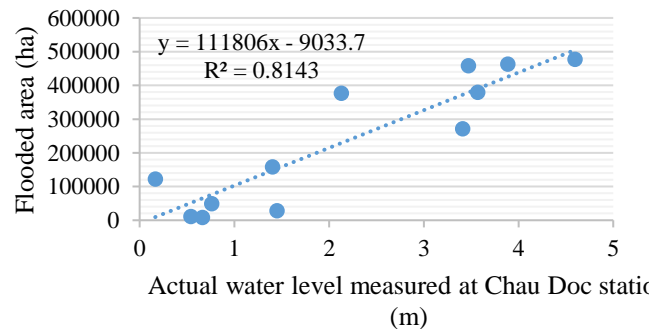


Figure 13: The correlation between the flooded area in the Tu Giac Long Xuyen and the observed water level in Chau Doc

The results from the graph show that there is a fairly good correlation between the flooded area in the Tu Giac Long Xuyen and water level monitoring data at Chau Doc station. Verification results show the coefficient $R^2 = 0.8143$ (Figure 13).

Compare the interpretation results with monitoring data at Xuan To measuring station.

The results from the graph show that there is a fairly good correlation between the flooded area in the Tu Giac Long Xuyen and water level monitoring data at Xuan To station. Verification results show the coefficient $R^2 = 0.8728$ (Figure 14).

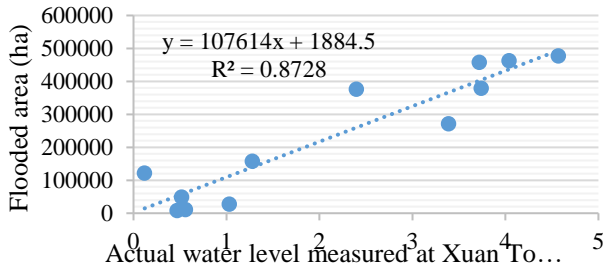


Figure 14: The correlation between the flooded area in the Tu Giac Long Xuyen and the observed water level in Xuan To

TABLE V

STATISTICS OF LANDSAT AND MODIS IMAGES

No	Name	Area Landsat	%	Area (MODIS)	%	Dev	Error (%)
1	Flooded areas	390,144.88	78.3	427276.87	85.37	37131	9.517

Comparing the analysis results between two images (Landsat 30m, MODIS 500m) with the above deviation ranging from 0 to 11% of the total interpreted area of the Landsat image, this deviation is completely acceptable. Because the accuracy of Landsat images is nearly 17 times greater than the accuracy of MODIS. From there it can be concluded that the same area but when interpreted in two different types of remote sensing images will produce different results. The accuracy of image interpretation depends on the accuracy of the interpreted image (Table 5).

IV. DISCUSSION

In the realm of environmental science, particularly in the study of flood impacts using remote sensing technology, the methodological rigor and the choice of

tools play a pivotal role in shaping the research outcomes. This discussion delves into the comparative strengths of Landsat and MODIS satellite systems, both integral to our study's methodology, and how these technologies have been harnessed to monitor and analyze flood dynamics comprehensively.

The core of our research strategy involves advanced processing techniques of Landsat and MODIS data. For Landsat, this encompasses the acquisition and precise correction of spectral data. Such meticulous corrections are crucial as they adjust for any sensor discrepancies and atmospheric disturbances, thereby enhancing the reliability of the imagery. Conversely, MODIS's frequent revisits provide a dynamic perspective on changing surface conditions, crucial during and post-flood events, thus complementing the detailed spatial analysis offered by Landsat.

Moreover, the application of sophisticated classification techniques, such as the Normalized Difference Water Index (NDWI) and the Enhanced Vegetation Index (EVI), plays a fundamental role. These indices are utilized to differentiate between water and non-water features and to assess vegetation health, which is often adversely affected by flooding. Employing these indices, alongside supervised classification methods using algorithms like Maximum Likelihood, allows for the creation of highly accurate and detailed flood maps.

This dual-satellite approach, integrating Landsat's high-resolution imagery with MODIS's rapid temporal data, equips us with a robust framework for environmental analysis. It not only bolsters our understanding of flood mechanisms but also significantly contributes to the development of more effective flood management strategies. These strategies aid policymakers and local authorities in making informed decisions, ultimately enhancing community resilience against such natural calamities.

In conclusion, the methodological sophistication embedded in our research underscores the importance of selecting appropriate remote sensing technologies and analytical techniques to address complex environmental issues. By leveraging the unique capabilities of both Landsat and MODIS, our study exemplifies a comprehensive and detailed approach to environmental monitoring, which is critical for mitigating the impacts of flooding and enhancing disaster preparedness.

V. CONCLUSIONS

Our study, centered on the application of Landsat and MODIS satellite imagery for flood impact assessment, has elucidated several key insights into the dynamics and extent of flood events. Through a meticulously crafted methodology, the integration of high-resolution spatial data from Landsat with the temporal accuracy provided by MODIS has enabled a comprehensive environmental analysis, demonstrating the vital role of advanced remote sensing technology in understanding and managing flood risks.

The rigorous data processing techniques employed, including radiometric and geometric corrections of the spectral data, have significantly enhanced the quality and reliability of the images. Moreover, the use of sophisticated classification algorithms, such as the Normalized Difference Water Index (NDWI) and the Enhanced Vegetation Index (EVI), has proven instrumental in accurately identifying water bodies and assessing flood extents. These methodologies have not only facilitated a detailed mapping of flood-prone areas but have also contributed to our understanding of how landscapes change in response to flooding.

In terms of practical applications, this research provides valuable insights for policymakers and disaster management teams. The detailed environmental data and flood maps produced can assist in developing more effective flood mitigation and

response strategies, ultimately aiding in the protection of vulnerable communities and ecosystems.

Overall, this study reinforces the importance of integrating various remote sensing tools and methodologies to achieve a detailed and dynamic understanding of environmental phenomena like flooding. Future research should continue to refine these methodologies, possibly integrating additional data sources or newer satellite technologies to further enhance the accuracy and applicability of flood impact assessments.

VI. REFERENCES

- [1]. Ahmed, M.R., et al. [3] Remote Sensing-Based Quantification of the Impact of Flash Flooding on the Rice Production: A Case Study over Northeastern Bangladesh. *Sensors*, 2017. 17, DOI: 10.3390/s17102347.
- [2]. Cianci, A., [8] Agrobiodiversity, agroecology, and private law. 2019. p. 31-36.
- [3]. Asare-Kyei, D., G. Forkuor, and V. Venus [6] Modeling Flood Hazard Zones at the Sub-District Level with the Rational Model Integrated with GIS and Remote Sensing Approaches. *Water*, 2015. 7, 3531-3564 DOI: 10.3390/w7073531.
- [4]. Dao, P., Y.-A. Liou, and C.-W. Chou, [9] Detection of Flood Inundation Regions with Landsat/MODIS Synthetic Data. 2015.
- [5]. Ahamed, A., et al., [1] Near Real-Time Flood Monitoring and Impact Assessment Systems, in *Remote Sensing of Hydrological Extremes*, V. Lakshmi, Editor. 2017, Springer International Publishing: Cham. p. 105-118.
- [6]. Irimescu, A., et al., [17] The use of remote sensing and GIS techniques in flood monitoring and damage assessment: a study case in Romania. 2015.
- [7]. Dao, P.D., N.T. Mong, and H.-P. Chan, [11] Landsat-MODIS image fusion and object-based

- image analysis for observing flood inundation in a heterogeneous vegetated scene. *GIScience & remote sensing*, 2019. 56(8): p. 1148-1169.
- [8]. Rahman, M. and L. Di, [26] [27] The state of the art of spaceborne remote sensing in flood management. *Natural Hazards*, 2017. 85.
- [9]. Ahmed, K.R. and S. Akter, [2] Analysis of landcover change in southwest Bengal delta due to floods by NDVI, NDWI and K-means cluster with landsat multi-spectral surface reflectance satellite data. *Remote Sensing Applications: Society and Environment*, 2017. 8: p. 168-181.
- [10]. Sadeghian, F., et al., [28] Effects of electrokinetic phenomena on the load-bearing capacity of different steel and concrete piles: A small-scale experimental study. *Canadian Geotechnical Journal*, 2020. 58.
- [11]. Ghorbani, M.A., et al., [13] Chaos-based multigene genetic programming: A new hybrid strategy for river flow forecasting. *Journal of Hydrology*, 2018. 562: p. 455-467.
- [12]. Mateus, S. and J. Branch, [22] Intelligent Virtual Environment Using Artificial Neural Networks. 2017. 43-53.
- [13]. Puspitasari, S., [25] Sampul Belakang. *Jurnal Penelitian Karet*, 2021: p. xviii-xxii.
- [14]. Landuyt, L., N.E. Verhoest, and F.M. Van Coillie, Flood mapping in vegetated areas using an unsupervised clustering approach on sentinel-1 and-2 imagery. *Remote Sensing*, 2020. 12(21): p. 3611.
- [15]. Li, K., J. Wang, and J. Yao, Effectiveness of machine learning methods for water segmentation with ROI as the label: A case study of the Tuul River in Mongolia. *International Journal of Applied Earth Observation and Geoinformation*, 2021. 103: p. 102497.
- [16]. Chander, G., et al., Monitoring on-orbit calibration stability of the Terra MODIS and Landsat 7 ETM+ sensors using pseudo-invariant test sites. *Remote Sensing of Environment*, 2010. 114(4): p. 925-939.
- [17]. Robinson, N.P., et al., A dynamic Landsat derived normalized difference vegetation index (NDVI) product for the conterminous United States. *Remote sensing*, 2017. 9(8): p. 863.
- [18]. Chander, G., D.J. Meyer, and D.L. Helder, Cross calibration of the Landsat-7 ETM+ and EO-1 ALI sensor. *IEEE Transactions on Geoscience and Remote Sensing*, 2004. 42(12): p. 2821-2831.
- [19]. Islam, K.A., et al., Flood detection using multi-modal and multi-temporal images: A comparative study. *Remote Sensing*, 2020. 12(15): p. 2455.
- [20]. Hidayah, E., et al., Flood mapping based on open-source remote sensing data using an efficient band combination system. 2022.
- [21]. Sivanpillai, R., et al., Rapid flood inundation mapping by differencing water indices from pre- and post-flood Landsat images. *Frontiers of Earth Science*, 2021. 15: p. 1-11.
- [22]. Rahmat, A., et al. Analysis of Normalized Different Wetness Index (NDWI) Using Landsat Imagery in the Ciletuh Geopark Area as Ecosystem Monitoring. in *IOP Conference Series: Earth and Environmental Science*. 2022. IOP Publishing.
- [23]. Ticehurst, C., et al. Using MODIS for mapping flood events for use in hydrological and hydrodynamic models: Experiences so far. in *20th international congress on modelling and simulation*, Adelaide, Australia. 2013.
- [24]. Khalifeh Soltanian, F., M. Abbasi, and H. Riyahi Bakhtyari, Flood monitoring using ndwi and mndwi spectral indices: A case study of aghqala flood-2019, Golestan Province, Iran. *The International Archives of the Photogrammetry, Remote Sensing and Spatial Information Sciences*, 2019. 42: p. 605-607.
- [25]. Kwak, Y., B. Arifuzzanman, and Y. Iwami, Prompt proxy mapping of flood damaged rice fields using MODIS-derived indices. *Remote Sensing*, 2015. 7(12): p. 15969-15988.

- [26]. Thy, P.T.M. and H.D. Duan, A Study On The Potential Of Applying Moderate Resolution Imaging Spectroradiometer (Modis) For Detecting Land Cover Change In The Mekong Delta.
- [27]. Son, N.-T., C.-F. Chen, and C.-R. Chen, Flood assessment using multi-temporal remotely sensed data in Cambodia. *Geocarto International*, 2021. 36(9): p. 1044-1059.
- [28]. Vichet, N., et al., MODIS-Based investigation of flood areas in Southern Cambodia from 2002–2013. *Environments*, 2019. 6(5): p. 57.
- [29]. Ji, L., et al., On the terminology of the spectral vegetation index $(NIR - SWIR)/(NIR + SWIR)$. *International journal of remote sensing*, 2011. 32(21): p. 6901-6909.
- [30]. Dangwal, N., et al., Monitoring of water stress in wheat using multispectral indices derived from Landsat-TM. *Geocarto International*, 2016. 31(6): p. 682-693.
- [31]. Gao, W., et al., [12] Analysis of flood inundation in ungauged basins based on multi-source remote sensing data. *Environmental Monitoring and Assessment*, 2018. 190(3): p. 129.
- [32]. Psychogios, A., et al., [24] Varieties of crisis and working conditions: A comparative study of Greece and Serbia. *European Journal of Industrial Relations*, 2019. 26: p. 095968011983710.
- [33]. Kabenge, M., et al., [18] Characterizing flood hazard risk in data-scarce areas, using a remote sensing and GIS-based flood hazard index. *Natural Hazards*, 2017. 89(3): p. 1369-1387.